

Improved Hysteresis and Reliability of MoS₂ Transistors With High-Quality CVD Growth and Al₂O₃ Encapsulation

Yury Yu. Illarionov¹, Kirby K. H. Smithe², Michael Waltl³, Theresia Knobloch,
Eric Pop, *Senior Member, IEEE*, and Tibor Grasser, *Fellow, IEEE*

Abstract—We report considerable improvement in the hysteresis and reliability of single-layer MoS₂ field-effect transistors (FETs) achieved by chemical vapor deposition (CVD) of MoS₂ and dielectric encapsulation. Our results show that a high-quality 15-nm thick Al₂O₃ layer allows for an efficient protection of the devices from adsorbent-type trapping sites. Combined use of the CVD-grown MoS₂ as a channel and encapsulation simultaneously leads to at least an order of magnitude smaller hysteresis and up to two orders of magnitude lower long-term drifts of the transistor characteristics. Together with high on/off current ratios ($\sim 10^9$) achieved in our devices, this presents a considerable advance in the technology of MoS₂ FETs. As such, we conclude that both CVD growth of MoS₂ and encapsulation present important technological steps toward reaching commercial quality standards of next-generation two-dimensional (2D) material technologies.

Index Terms—Single-layer MoS₂, encapsulation, reliability, charged traps, hysteresis, bias-temperature instabilities.

I. INTRODUCTION

MOLYBDENUM disulfide (MoS₂) is now considered a promising “beyond-graphene” material for applications in next-generation two-dimensional (2D) electronics. In contrast to graphene, MoS₂ has a sizable direct electronic bandgap of up to ~ 2.6 eV in the single-layer limit [1]–[3], which makes this material attractive for digital device applications. Owing to this, considerable progress in fabrication of single-layer (1L) MoS₂ field-effect transistors (FETs) has been demonstrated recently. In particular, numerous single-layer devices with SiO₂ [4], [5], Al₂O₃ [6], HfO₂ [4] and hexagonal boron nitride (hBN) [7], [8] gate insulators have

been reported. The typical on/off current ratios of these devices are within 10^5 – 10^7 , while the subthreshold swing (SS) can reach nearly ideal values down to 74 mV/dec, as already reported for high-k/MoS₂/SiO₂ devices [4]. In addition, a number of successful attempts at fabricating multi-layer MoS₂ FETs have been undertaken [9]–[17], with the best subthreshold swing of 69 mV/dec achieved for MoS₂/high-k devices [17]. However, independent of the number of channel layers, available MoS₂ device prototypes often suffer from a sizable hysteresis [5], [8], [10], [14], [15] and long-term drifts of the gate transfer characteristics [8], [11], [13], which are known from Si technologies as bias-temperature instabilities (BTI) [18]–[20]. These issues are typically attributed to charge trapping by both oxide traps [8], [13], [15] and adsorbent-type trapping sites (e.g. water molecules) on the MoS₂ channel [5], [8], [10], [11]. While the hysteresis and BTI impede stable device operation at a defined operating point, the reliability of MoS₂ prototypes with respect to these issues is still far below the standards of modern commercial FETs [8], [11], [13]. As such, BTI and hysteresis in MoS₂ FETs must be addressed prior to commercialization of these next-generation technologies.

Here we report on the improvement of both the reliability and the performance of 1L MoS₂ FETs with SiO₂ insulator by optimized device processing and encapsulation with a high-quality 15 nm thick Al₂O₃ layer. Our results show that these devices not only exhibit high on/off current ratio ($\sim 10^9$), but also that both the hysteresis and the threshold voltage shifts due to positive and negative BTI (PBTI and NBTI, respectively) become 1–2 orders of magnitude smaller. Combined with the use of CVD-grown MoS₂, this presents a considerable breakthrough in the technology of 2D single-layer materials and devices.

II. DEVICES

Our devices are single-layer back-gated MoS₂ FETs with a 25 nm thick SiO₂ insulator, 50 nm thick gold source/drain contacts and a 15 nm thick high-quality Al₂O₃ encapsulation (Fig. 1a,b). Single-layer MoS₂ was grown at $T = 850$ °C in Ar atmosphere (760 Torr) by chemical vapor deposition (CVD) directly on SiO₂/p⁺⁺–Si substrates [21]; growth time was 15 minutes. Then, after verification of the superior quality of our CVD-grown MoS₂ film [22], the MoS₂ FETs were fabricated via a three-step optical lithography process to

Manuscript received October 6, 2017; accepted October 28, 2017. Date of publication November 1, 2017; date of current version November 22, 2017. This work was supported by the FWF under Grant I2606-N30. The work of K. K. H. Smithe and E. Pop was supported in part by the NSF EFRI 2-DARE Grant 154288 and in part by the AFOSR Grant FA9550-14-1-0251. The review of this letter was arranged by Editor K. Uchida. (Corresponding author: Yury Yu. Illarionov.)

Y. Y. Illarionov is with the Institut für Mikroelektronik der TU Wien, 1040 Vienna, Austria, and also with the Ioffe Physical-Technical Institute, 194021 St-Petersburg, Russia (e-mail: illarionov@iue.tuwien.ac.at).

M. Waltl, T. Knobloch, and T. Grasser are with the Institut für Mikroelektronik der TU Wien, 1040 Vienna, Austria.

K. K. H. Smithe and E. Pop are with the Department of Electrical Engineering, Stanford University, Stanford, CA 94305 USA.

Color versions of one or more of the figures in this letter are available online at <http://ieeexplore.ieee.org>.

Digital Object Identifier 10.1109/LED.2017.2768602

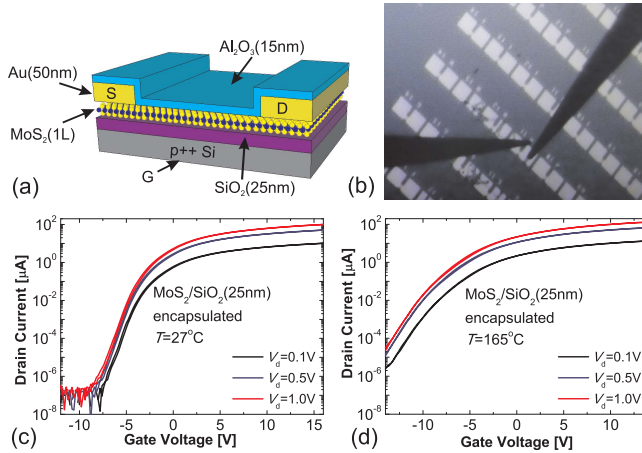


Fig. 1. (a) Schematic layout of our CVD-grown 1L MoS₂ FETs encapsulated by a 15 nm thick Al₂O₃ layer. (b) Optical microscope image of the investigated devices (the contact pads are 100 × 100 μm²). The $I_D - V_G$ characteristics of our device ($L = 8 \mu\text{m}$, $W = 20 \mu\text{m}$) measured at $T = 27^\circ\text{C}$ (c) and $T = 165^\circ\text{C}$ (d).

simultaneously create hundreds of devices with channel dimensions ranging from 2 to 20 μm [22]. First, probe pad areas were defined with photoresist, etched out with O₂ plasma and filled with 2/40 nm Ti/Au. Following liftoff, contact extension regions were defined and filled with 50 nm of pure Au, in order to minimize contact resistance [23]. After a second liftoff, the channel widths were defined and the exposed MoS₂ was etched away with O₂ plasma, followed by a solvent clean to remove the photoresist. Finally, a high-quality Al₂O₃ encapsulation layer was deposited using a modified method of [24]. Namely, 120 cycles of atomic layer deposition (ALD) of Al₂O₃ were performed at 300 °C after deposition of a 1.5 nm thick Al nucleation layer. Note that a relatively high ALD growth temperature allows to remove impurities that might be present on the surface of the MoS₂ channel before deposition of the encapsulation layer. This Stanford-built ALD setup allows to deposit a high-quality Al₂O₃ layer with few inherent charge traps.

III. EXPERIMENTAL DETAILS

Electrical measurements were performed in a vacuum ($\sim 5 \times 10^{-6}$ Torr) in complete darkness. This was necessary to obtain consistent results for comparison with bare devices which are known to be sensitive to the detrimental impact of environment [5], [10]. First, we measured the drain current vs. gate voltage ($I_D - V_G$) characteristics using the autorange mode, which was necessary to evaluate the best case on/off current ratio in our devices. Then we analyzed the hysteresis dynamics by measuring the $I_D - V_G$ characteristics using forward (V^+) and reversed (V^-) sweep directions and different measurement frequencies $f = 1/(Nt_{\text{step}})$, with N being the number of V_G steps and t_{step} the sampling time [8]. Finally, we examined the BTI degradation and recovery dynamics using our experimental technique by applying subsequent stress/recovery cycles with logarithmically increased stress times t_s [8], [25]. A considerable difference compared to our previous work for MoS₂ FETs [8] is that, similarly to the technique used for Si devices [26], here a constant gate voltage is applied not only during stress (V_{GS}), but also

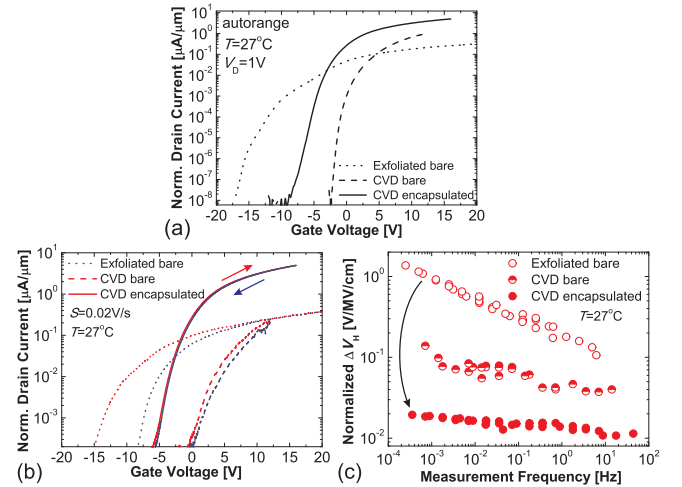


Fig. 2. (a) The $I_D - V_G$ characteristics of exfoliated MoS₂/SiO₂(90 nm) FET ($L = 1.5 \mu\text{m}$, $W = 7 \mu\text{m}$) and CVD-grown MoS₂/SiO₂(25 nm) devices ($L = 6 \mu\text{m}$, $W = 10 \mu\text{m}$ for bare and $L = 8 \mu\text{m}$, $W = 20 \mu\text{m}$ for encapsulated device) measured using the autorange mode. The current is normalized by W . (b) The $I_D - V_G$ characteristics of the same devices measured using both sweep directions and a constant sweep rate $S = 0.02 \text{ V/s}$. (c) The normalized hysteresis widths versus the measurement frequency f .

during recovery (V_{GR}). This leads to more reproducible results, as otherwise the potential at the back gate, which is formed by the Si substrate, shows large uncontrollable drifts.

IV. RESULTS AND DISCUSSION

In Fig. 1c we show the $I_D - V_G$ characteristics measured for our encapsulated CVD-grown MoS₂ device at $T = 27^\circ\text{C}$. The on/off current ratio is at least 10^9 , which is larger than previously reported for CVD-grown MoS₂. Also, similarly to our previous work on bare exfoliated MoS₂ FETs [8], at $T = 165^\circ\text{C}$ (Fig. 1d) the threshold voltage V_{th} of the same device becomes more negative. However, here this issue is less pronounced and thus the measured on/off current ratio remains as high as 10^7 , which further underlines the high stability of these encapsulated CVD-grown devices.

In Fig. 2a, b we compare the $I_D - V_G$ characteristics measured for our encapsulated CVD-grown MoS₂/SiO₂(25 nm) devices, bare devices fabricated using the same method, and bare exfoliated single-layer MoS₂/SiO₂(90 nm) FETs which are similar to those studied in our previous work [8]. Owing to improved processing technology, CVD-grown devices exhibit considerably steeper subthreshold slopes and larger on current values. Furthermore, the hysteresis, which is sizable for bare exfoliated devices, becomes considerably smaller for bare CVD-grown devices and can be almost completely suppressed for their encapsulated counterparts. In Fig. 2c we compare the hysteresis widths ΔV_H normalized by the oxide field factor $(V_{G_{\text{max}}} - V_{G_{\text{min}}})/d_{\text{ox}}$, with d_{ox} being the oxide thickness, versus the measurement frequency f for three devices. Clearly, the encapsulated CVD-grown device exhibits nearly one order of magnitude improvement compared to a bare device of the same technology and two orders of magnitude compared to the exfoliated bare device. As such, we can conclude that our high-quality Al₂O₃ encapsulation layer efficiently protects the devices from fast adsorbent-type trapping sites which are in part responsible for the hysteresis in MoS₂ FETs.

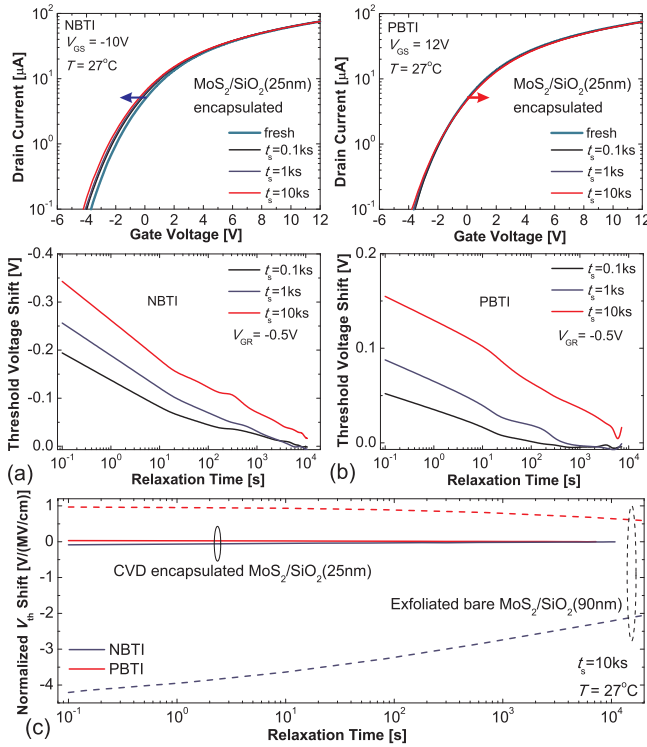


Fig. 3. Evolution of the $I_D - V_G$ characteristics of our encapsulated CVD-grown MoS₂ FET with $L = 8 \mu\text{m}$, $W = 20 \mu\text{m}$ (top) and the corresponding V_{th} recovery traces (bottom) after subsequent NBTI (a) and PBTI (b) stresses. (c) Normalized NBTI and PBTI recovery measured after $t_s = 10$ ks stresses.

In Fig. 3a,b we show evolution of the $I_D - V_G$ characteristics and corresponding V_{th} recovery traces measured at the recovery gate voltage $V_{GR} = -0.5$ V after subsequent NBTI and PBTI stresses. Remarkably, the degradation is considerably smaller than has been ever reported for MoS₂ FETs. In particular, in Fig. 3c we compare the NBTI and PBTI recovery traces measured after stresses with $t_s = 10$ ks for our encapsulated CVD-grown MoS₂ FETs and their bare exfoliated counterparts from our previous work [8]. Since the oxide thicknesses and stress voltages are different, we normalize the threshold voltage shifts by the oxide field $F_{ox} = V_{GS}/d_{ox}$, which is 2.2 MV/cm for exfoliated device and either 4 MV/cm (NBTI) or 4.8 MV/cm (PBTI) for CVD-grown MoS₂ FET. While for encapsulated CVD-grown devices both NBTI and PBTI shifts are more than an order of magnitude smaller, they tend to completely recover after several hours. In contrast, the degree of recovery of considerable BTI shifts in bare exfoliated MoS₂ FETs for the same time interval does not exceed 40%. Therefore, we conclude that Al₂O₃ encapsulation, together with our optimized device processing, allows to minimize the amount of slower process-induced defects and adsorbents, which may contribute to charge trapping leading to BTI. As such, we suggest that the observed BTI degradation in our encapsulated devices is dominated by oxide traps in SiO₂, which are situated within several nanometers from the MoS₂/SiO₂ interface and thus can exchange charges with the channel by means of tunneling. As known from Si technologies [27] and our previous works on black phosphorus (BP) [28] and MoS₂ FETs [29], these defects are

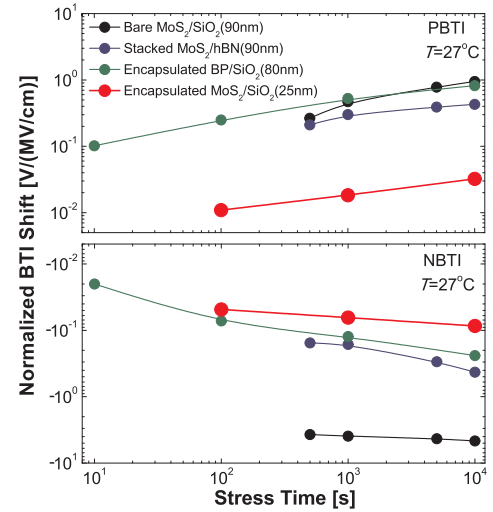


Fig. 4. Comparison of the PBTI (top) and NBTI (bottom) shifts normalized by the oxide field (0.4–4.8 MV/cm) for different 2D technologies. Encapsulated CVD-grown MoS₂/SiO₂ FETs exhibit the best NBTI and PBTI reliability.

energetically aligned within certain defect bands, with the one contributing to charge trapping in MoS₂ FETs located ~ 2.7 eV below the SiO₂ conduction band edge [27], [28]. This position of the defect band relative to the MoS₂ conduction band, together with the Fermi level pinning in accumulation [30], [31], makes NBTI more favorable than PBTI. That is why PBTI degradation in our devices is weaker than NBTI, which is important for MoS₂ n-FETs working at positive V_G .

Finally, in Fig. 4 we compare initially measured normalized PBTI and NBTI shifts versus t_s for our encapsulated CVD-grown MoS₂/SiO₂ FETs with those obtained for bare exfoliated MoS₂/SiO₂ [8], stacked MoS₂/hBN [8] and BP/SiO₂ [28] devices. Remarkably, the PBTI shifts for our encapsulated MoS₂ FETs are around an order of magnitude smaller than in previously studied 2D devices. As for NBTI, encapsulated MoS₂ devices studied here can slightly outperform Al₂O₃ encapsulated BP/SiO₂ FETs, which have been previously considered the most stable with respect to room temperature BTI among other 2D devices. Although commercial standards require further improvement of the reliability by at least one order of magnitude, our encapsulated MoS₂ FETs present a considerable step forward in this direction.

V. CONCLUSIONS

In summary, we have suggested a versatile way to improve both the reliability and performance of MoS₂ FETs by optimization of the device processing conditions and the use of a high-quality Al₂O₃ encapsulation to protect the devices from adsorbent-type trapping sites. While already having an extremely high on/off current ratio of $\sim 10^9$, our devices also exhibit a considerable improvement in terms of hysteresis and BTI stability. As such, we conclude that high-quality encapsulation of MoS₂ FETs, together with CVD growth of MoS₂ film, present an important technological step toward reaching commercial quality standards of these new technologies.

REFERENCES

- [1] A. R. Klots, A. K. M. Newaz, B. Wang, D. Prasai, H. Krzyzanowska, J. Lin, D. Caudel, N. J. Ghimire, J. Yan, B. L. Ivanov, K. A. Velizhanin, A. Burger, D. G. Mandrus, N. H. Tolk, S. T. Pantelides, and K. I. Bolotin, "Probing excitonic states in suspended two-dimensional semiconductors by photocurrent spectroscopy," *Sci. Rep.*, vol. 4, Oct. 2014, Art. no. 6608, doi: [10.1038/srep06608](https://doi.org/10.1038/srep06608).
- [2] Y. Huang, Y. Chen, W. Zhang, S. Quek, C.-H. Chen, L.-J. Li, W.-T. Hsu, W.-H. Chang, Y. Zheng, W. Chen, and A. Wee, "Bandgap tunability at single-layer molybdenum disulfide grain boundaries," *Nature Commun.*, vol. 6, Aug. 2015, Art. no. 6298, doi: [10.1038/ncomms7298](https://doi.org/10.1038/ncomms7298).
- [3] F. A. Rasmussen and K. S. Thygesen, "Computational 2D materials database: Electronic structure of transition-metal dichalcogenides and oxides," *J. Phys. Chem. C*, vol. 119, no. 23, pp. 13169–13183, Apr. 2015, doi: [10.1021/acs.jpcc.5b02950](https://doi.org/10.1021/acs.jpcc.5b02950).
- [4] B. Radisavljevic, A. Radenovic, J. Brivio, V. Giacometti, and A. Kis, "Single-layer MoS₂ transistors," *Nature Nanotechnol.*, vol. 6, no. 3, pp. 147–150, 2011, doi: [10.1038/nnano.2010.279](https://doi.org/10.1038/nnano.2010.279).
- [5] D. J. Late, B. Liu, H. S. S. R. Matte, V. P. Dravid, and C. N. R. Rao, "Hysteresis in single-layer MoS₂ field effect transistors," *ACS Nano*, vol. 6, no. 6, pp. 5635–5641, Jun. 2012, doi: [10.1021/nl301572c](https://doi.org/10.1021/nl301572c).
- [6] J. Kang, W. Liu, and K. Banerjee, "High-performance MoS₂ transistors with low-resistance molybdenum contacts," *Appl. Phys. Lett.*, vol. 104, no. 9, p. 093106, Mar. 2014, doi: [10.1063/1.4866340](https://doi.org/10.1063/1.4866340).
- [7] G.-H. Lee, Y.-J. Yu, X. Cui, N. Petrone, C.-H. Lee, M. Choi, D.-Y. Lee, C. Lee, W. Yoo, K. Watanabe, T. Taniguchi, C. Nockolls, P. Kim, and J. Hone, "Flexible and transparent MoS₂ field-effect transistors on hexagonal boron nitride-graphene heterostructures," *ACS Nano*, vol. 7, no. 9, pp. 7931–7936, Aug. 2013, doi: [10.1021/nl402954e](https://doi.org/10.1021/nl402954e).
- [8] Y. Y. Illarionov, G. Rzepa, M. Waltl, T. Knobloch, A. Grill, M. M. Furchi, T. Mueller, and T. Grasser, "The role of charge trapping and MoS₂/SiO₂ and MoS₂/hBN field-effect transistors," *2D Mater.*, vol. 3, no. 3, p. 035004, Jul. 2016, doi: [10.1088/2053-1583/3/3/035004](https://doi.org/10.1088/2053-1583/3/3/035004).
- [9] S. Das, H.-Y. Chen, A. V. Penumatcha, and J. Appenzeller, "High performance multilayer MoS₂ transistors with scandium contacts," *Nano Lett.*, vol. 13, no. 1, pp. 100–105, 2012, doi: [10.1021/nl303583v](https://doi.org/10.1021/nl303583v).
- [10] H. Qiu, L. Pan, Z. Yao, J. Li, Y. Shi, and X. Wang, "Electrical characterization of back-gated bi-layer MoS₂ field-effect transistors and the effect of ambient on their performances," *Appl. Phys. Lett.*, vol. 100, no. 12, p. 123104, Mar. 2012, doi: [10.1063/1.3696045](https://doi.org/10.1063/1.3696045).
- [11] K. Cho, W. Park, J. Park, H. Jeong, J. Jang, T.-Y. Kim, W.-K. Hong, S. Hong, and T. Lee, "Electric stress-induced threshold voltage instability of multilayer MoS₂ field effect transistors," *ACS Nano*, vol. 7, no. 9, pp. 7751–7758, Aug. 2013, doi: [10.1021/nl402348r](https://doi.org/10.1021/nl402348r).
- [12] T. Li, G. Du, B. Zhang, and Z. Zeng, "Scaling behavior of hysteresis in multilayer MoS₂ field effect transistors," *Appl. Phys. Lett.*, vol. 105, no. 9, p. 093107, Sep. 2014, doi: [10.1063/1.4894865](https://doi.org/10.1063/1.4894865).
- [13] S. Yang, S. Park, S. Jang, H. Kim, and J.-Y. Kwon, "Electrical stability of multilayer MoS₂ field-effect transistor under negative bias stress at various temperatures," *Phys. Status Solidi RRL*, vol. 8, no. 8, pp. 714–718, Aug. 2014, doi: [10.1002/pssr.201409146](https://doi.org/10.1002/pssr.201409146).
- [14] A.-J. Cho, S. Yang, K. Park, S. D. Namgung, H. Kim, and J.-Y. Kwon, "Multi-layer MoS₂ FET with small hysteresis by using atomic layer deposition Al₂O₃ as gate insulator," *ECS Solid State Lett.*, vol. 3, no. 10, pp. Q67–Q69, Aug. 2014, doi: [10.1149/2.0111409ssl](https://doi.org/10.1149/2.0111409ssl).
- [15] Y. Guo, X. Wei, J. Shu, B. Liu, J. Yin, C. Guan, Y. Han, S. Gao, and Q. Chen, "Charge trapping at the MoS₂-SiO₂ interface and its effects on the characteristics of MoS₂ metal-oxide-semiconductor field effect transistors," *Appl. Phys. Lett.*, vol. 106, no. 10, p. 103109, Mar. 2015, doi: [10.1063/1.4914968](https://doi.org/10.1063/1.4914968).
- [16] K. L. Ganapathi, S. Bhattacharjee, S. Mohan, and N. Bhat, "High-performance HfO₂ back gated multilayer MoS₂ transistors," *IEEE Electron Device Lett.*, vol. 37, no. 6, pp. 797–800, Apr. 2016, doi: [10.1109/LED.2016.2553059](https://doi.org/10.1109/LED.2016.2553059).
- [17] P. Bolshakov, P. Zhao, A. Azcatl, P. K. Hurley, R. M. Wallace, and C. D. Young, "Electrical characterization of top-gated molybdenum disulfide field-effect-transistors with high-*k* dielectrics," *Microelectron. Eng.*, vol. 178, pp. 190–193, Jun. 2017, doi: [10.1016/j.mee.2017.04.045](https://doi.org/10.1016/j.mee.2017.04.045).
- [18] V. Huard, "Two independent components modeling for negative bias temperature instability," in *Proc. IEEE Int. Rel. Phys. Symp. (IRPS)*, May 2010, pp. 33–42, doi: [10.1109/IRPS.2010.5488857](https://doi.org/10.1109/IRPS.2010.5488857).
- [19] D. S. Ang, Z. Q. Teo, T. J. J. Ho, and C. M. Ng, "Reassessing the mechanisms of negative-bias temperature instability by repetitive stress/relaxation experiments," *IEEE Trans. Device Mater. Rel.*, vol. 11, no. 1, pp. 19–34, Mar. 2011, doi: [10.1109/TDMR.2010.2067216](https://doi.org/10.1109/TDMR.2010.2067216).
- [20] T. Grasser, "Stochastic charge trapping in oxides: From random telegraph noise to bias temperature instabilities," *Microelectron. Rel.*, vol. 52, no. 1, pp. 39–70, Jan. 2012, doi: [10.1016/j.microrel.2011.09.002](https://doi.org/10.1016/j.microrel.2011.09.002).
- [21] K. K. H. Smithe, C. D. English, S. V. Suryavanshi, and E. Pop, "Intrinsic electrical transport and performance projections of synthetic monolayer MoS₂ devices," *2D Mater.*, vol. 4, no. 1, p. 011009, 2017, doi: [10.1088/2053-1583/4/1/011009](https://doi.org/10.1088/2053-1583/4/1/011009).
- [22] K. K. H. Smithe, S. V. Suryavanshi, M. Muñoz-Rojo, A. D. Tedjarati, and E. Pop, "Low variability in synthetic monolayer MoS₂ devices," *ACS Nano*, vol. 11, no. 8, pp. 8456–8463, Jul. 2017, doi: [10.1021/acsnano.7b04100](https://doi.org/10.1021/acsnano.7b04100).
- [23] C. D. English, G. Shine, V. E. Dorgan, K. C. Saraswat, and E. Pop, "Improved contacts to MoS₂ transistors by ultra-high vacuum metal deposition," *Nano Lett.*, vol. 16, no. 6, pp. 3824–3830, May 2016, doi: [10.1021/acs.nanolett.6b01309](https://doi.org/10.1021/acs.nanolett.6b01309).
- [24] M. J. Mleczko, R. L. Xu, K. Okabe, H.-H. Kuo, I. R. Fisher, H.-S. P. Wong, Y. Nishi, and E. Pop, "High current density and low thermal conductivity of atomically thin semimetallic WTe₂," *ACS Nano*, vol. 10, no. 8, pp. 7507–7514, Jul. 2016, doi: [10.1021/acsnano.6b02368](https://doi.org/10.1021/acsnano.6b02368).
- [25] Y. Y. Illarionov, A. D. Smith, S. Vaziri, M. Ostling, T. Mueller, M. C. Lemme, and T. Grasser, "Bias-temperature instability in single-layer graphene field-effect transistors," *Appl. Phys. Lett.*, vol. 105, no. 14, p. 143507, Oct. 2014, doi: [10.1063/1.4897344](https://doi.org/10.1063/1.4897344).
- [26] T. Grasser, P.-J. Wagner, H. Reisinger, T. Aichinger, G. Pobegen, M. Nelhiebel, and B. Kaczer, "Analytic modeling of the bias temperature instability using capture/emission time maps," in *IEDM Tech. Dig.*, Dec. 2011, pp. 27.4.1–27.4.4, doi: [10.1109/IEDM.2011.6131624](https://doi.org/10.1109/IEDM.2011.6131624).
- [27] R. Degraeve, M. Cho, B. Govoreanu, B. Kaczer, M. B. Zahid, J. Van Houdt, M. Jurczak, and G. Groeseneken, "Trap spectroscopy by charge injection and sensing (TSCIS): A quantitative electrical technique for studying defects in dielectric stacks," in *IEDM Tech. Dig.*, Dec. 2008, pp. 1–4, doi: [10.1109/IEDM.2008.4796812](https://doi.org/10.1109/IEDM.2008.4796812).
- [28] Y. Y. Illarionov, M. Waltl, G. Rzepa, J.-S. Kim, S. Kim, A. Dodabalapur, D. Akinwande, and T. Grasser, "Long-term stability and reliability of black phosphorus field-effect transistors," *ACS Nano*, vol. 10, no. 10, pp. 9543–9549, Oct. 2016, doi: [10.1021/acsnano.6b04814](https://doi.org/10.1021/acsnano.6b04814).
- [29] Y. Y. Illarionov, T. Knobloch, M. Waltl, G. Rzepa, A. Pospisichil, D. K. Polyushkin, M. M. Furchi, T. Mueller, and T. Grasser, "Energetic mapping of oxide traps in MoS₂ field-effect transistors," *2D Mater.*, vol. 4, no. 2, p. 025108, Jun. 2017, doi: [10.1088/2053-1583/aa734a](https://doi.org/10.1088/2053-1583/aa734a).
- [30] C. Gong, L. Colombo, R. M. Wallace, and K. Cho, "The unusual mechanism of partial Fermi level pinning at metal–MoS₂ interfaces," *Nano Lett.*, vol. 14, no. 4, pp. 1714–1720, Mar. 2014, doi: [10.1021/nl403465v](https://doi.org/10.1021/nl403465v).
- [31] H. Liu, M. Si, Y. Deng, A. Neal, Y. Du, S. Najmaei, P. M. Ajayan, J. Lou, and P. D. Ye, "Switching mechanism in single-layer molybdenum disulfide transistors: An insight into current flow across Schottky barriers," *ACS Nano*, vol. 8, no. 1, pp. 1031–1038, Dec. 2014, doi: [10.1021/nl405916t](https://doi.org/10.1021/nl405916t).